

Substorm observations in Apatity during 2012/13 winter season: a case study

Veneta Guineva¹, Irina Despirak², Boris Kozelov²

¹Space Research and Technology Institute, BAS, Stara Zagora, Bulgaria

²Polar Geophysical Institute, RAS, Apatity, Murmansk region, Russia

E mail (v_guineva@yahoo.com).

Accepted: 27 March 2015

Abstract All-sky camera data obtained at Apatity (Kola Peninsula) during 2012/2013 winter season and during December 2013 have been used to study the variation of substorm development during different conditions of the interplanetary medium. Solar wind and interplanetary magnetic field (IMF) parameters were taken from CDAWeb (http://cdaweb.gsfc.nasa.gov/cdaweb/istp_public/). Using WIND satellite data for the examined periods, the different solar wind streams were revealed: high speed streams from coronal magnetic holes (HSS) and magnetic clouds (MC) connected with non-stationary processes at the Sun. It is known that these solar wind structures are the sources of geomagnetic storms. Furthermore, the storms originating from these sources differ in intensity, recovery phase duration etc. We investigated substorm development during storms and during quiet conditions. Substorm onset time and further development were verified by ground-based data of IMAGE magnetometers network and Apatity all-sky camera. The particularities in the behaviour of substorms observed during storms and during quiet conditions are discussed.

© 2015 BBSCS RN SWS. All rights reserved

Key words: solar wind, substorms, auroras, westward electrojet

Introduction

It is known that during the expansion phase of a substorm, the auroras and westward electrojet propagate poleward (Akasofu (1964); Troshichev et al., 1974; Kisabeth and Rostoker, 1974; Wiens and Rostoker, 1975). The polar boundary of the auroras propagates poleward through a series of microsubstorms and intensifications, as well as the polar boundary of the electrojet moves poleward as a series of steplike jumps (Wiens and Rostoker, 1975; Sergeev and Yahnin, 1979).

The substorm appearance and development depend on the conditions in the solar wind (Akasofu et al., 1971, 1973; Lui et al., 1975, 1976; Petrukovich et al., 2000; Weatherwax et al., 1997; Gussenhofen, 1982; Yahnin et al., 2004). Studies were carried out on the influence of different geoeffective parameters of the solar wind and interplanetary magnetic field (IMF) (IMF Bz component, solar wind flow speed etc.) on the position of the auroras boundaries during substorms (e.g., Vorobjev and Zverev, 1982), on the latitude of the substorm onset (e.g., Gerard et al., 2004), on the substorm appearance at high geomagnetic latitudes (Akasofu, 2004; Gupta and Loomer, 1979; Loomer and Gupta, 1980; Sergeev, Yakhnin and Dmitrieva, 1979; Doolittle et al., 1998; Kuznetsov et al., 2001; Mende et al., 1999; Despirak et al., 2008; Despirak et al., 2009; Despirak, Lyubchich and Kleimenova, 2014).

It should be noted that it is important to consider the interplanetary parameters that are characteristic for different solar wind streams and structures in combination but not the solar wind effect separately. It is known that different combinations of geoeffective parameters (velocity, density, the Bz component of IMF, etc.) are typical for solar wind streams different in nature (e.g. Yermolaev et al., 2009). So, for recurrent

high speed solar wind streams (HSS) high velocities and low values of the negative Bz component of IMF are typical characteristics (see e.g., Tsurutani et al., 2006). The magnetic clouds (MCs) have high magnetic field values with long interval of negative Bz component of IMF and also increased values of plasma velocity (Klein and Burlaga, 1982; Burlaga et al., 1982). The compressed plasma regions in front of these streams, HSS and MC (the co-rotating interaction region (CIR) and Sheath region, respectively) are characterized by high solar wind density and a high magnitude of the magnetic field (Balogh et al., 1999).

It is also known that these three types of solar wind structures: MC, CIR and Sheath, are usually reasons of geomagnetic storms that differ by their main characteristics depending on the generating structure (e.g. Yermolaev and Yermolaev, 2006; Tsurutani et al., 2006). Therefore, substorms could be observed under different interplanetary conditions: during the passage of different solar wind streams and structures by the Earth, during development of different geomagnetic storms, as well as in quiet conditions.

In this paper we are presenting substorm observations in Apatity under different interplanetary conditions. Apatity is situated at auroral latitudes. Its geographic coordinates are: 67.58°N, 33.31°E and the corrected geomagnetic ones – 63.86°N, 112.9°E. This location is expedient to examine the variety of substorms.

Instrumentation and data used

All-sky camera data registered at Apatity during the 2012/2013 winter season and December 2013 have been used. The all-sky camera has been installed in Apatity since 2008 as a part of the observational system MAIN (Multiscale Aurora Imaging Network). It

comprises 4 auroral cameras with different fields of view providing simultaneous observations from spatially separated points. The cameras characteristics, their mutual situation and the measurement process are described in detail by Kozelov et al. (2011) and Kozelov et al. (2012).

Solar wind and interplanetary magnetic field parameters were taken from CDAWeb (http://sdaweb.gsfc.nasa.gov/cdaweb/istp_public/). OMNI data base revealed different solar wind streams: high speed recurrent streams from coronal magnetic holes (HSS) and magnetic clouds (MC) or quiet conditions for the examined periods.

Substorm onset time and further development were verified by data of Apatity all-sky camera and by ground-based data of IMAGE magnetometers network (using meridional chain Nurmijarvi (NUR) - Ny Alesund (NAL)), Lovozero and Loparskaya magnetometers.

The measurements during 2012/2013 season were examined together with the interplanetary conditions during the measuring periods. During the winter observational season, from October 2012 to March 2013, 4 magnetic clouds (MC) and 7 high speed recurrent streams (HSS) were detected. Some of them triggered geomagnetic storms. During the storm development and under quiet conditions the Apatity all-sky camera registered 40 substorm disturbances (substorms and their intensifications).

Below we are going to present 4 typical examples of substorm observations in Apatity: during a magnetic cloud under highly disturbed conditions, during a high speed recurrent stream under disturbed conditions and under quiet conditions.

Observations

Case 1: 17.03.2013

On 17.03.2013 a magnetic cloud passed by the Earth, and a geomagnetic storm with $D_{st} \sim -140$ nT developed. We considered substorms observations during the highly disturbed period, 17-18 March 2013, in Apatity.

Figure 1 shows the solar wind conditions taken from the OMNI database for the magnetic cloud on 17-18 March 2013. In Figure 1 from top to bottom the Interplanetary Magnetic Field magnitude (B_T), the IMF Z-component (B_Z), the flow velocity (V), the X-component of the velocity (V_x), the solar wind density (N), temperature (T), dynamic pressure (P), and the ground-based index SYM/H are shown. The time period of the magnetic cloud (MC) (15 UT, 17 March – 6 UT, 18 March 2013) and the region of interaction of MC with the undisturbed solar wind (Sheath) (06-15 UT on 17 March 2013) are marked as blue and red crosshatched areas, respectively. A geomagnetic storm developed during this time. The D_{st} index reached ~ -140 nT. Under these highly disturbed conditions, during the main phase of the storm, two substorms were observed at 18:26 UT and 18:39 UT, 17 March 2013 by the all-sky camera in Apatity. The onset times of these substorms are marked by black dashed vertical lines.

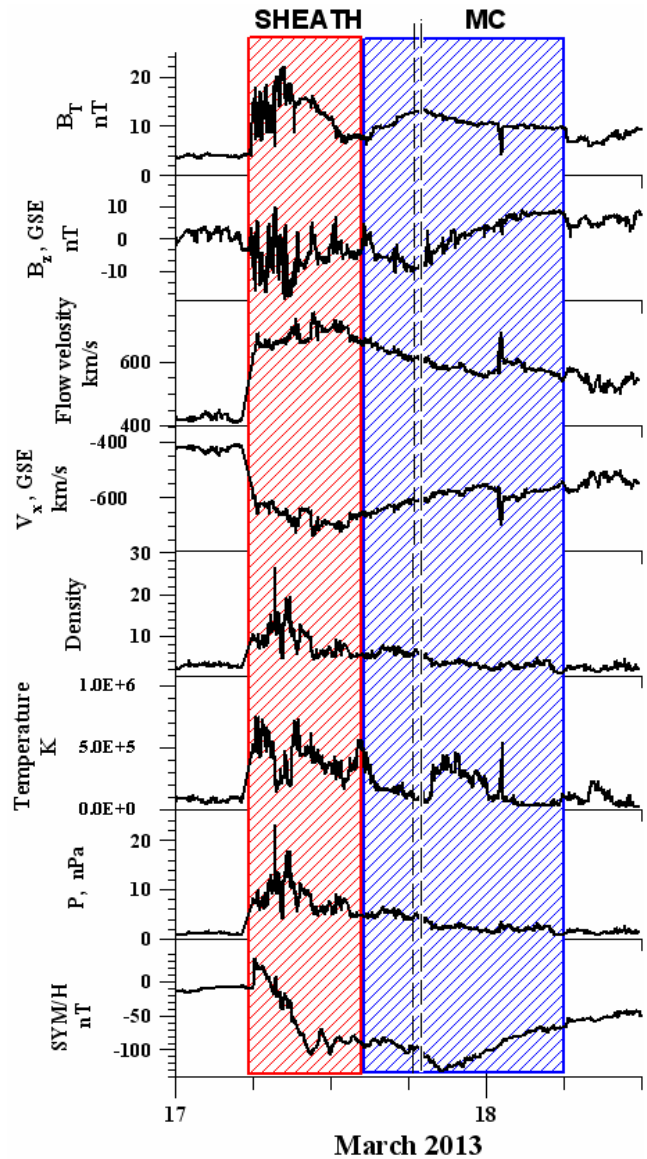


Figure 1 Event on 17 March 2013 - Magnetic cloud. Solar wind observations are presented: parameters of the solar wind and IMF (B_T , B_Z , V , V_x , N , T , P), and SYM/H index for the magnetic cloud on 17-18 March 2013. The magnetic cloud (MC) and Sheath regions are shown by shaded blue (to the right) and red (to the left) rectangles, respectively. The onsets of the substorms according IMAGE and all-sky camera are marked by dashed vertical lines.

In Figure 2 observations of substorm westward electrojet development by IMAGE magnetometers chain are presented. The left panel (2a) demonstrates the variations in the X-component of the magnetic field from 12 UT to 24 UT on 17 March 2013; the right panel (2b) shows the variations in the Z-component of the magnetic field from 12 UT to 24 UT. In this day 2 substorms were observed: at 18:25 UT and 18:40 UT. The oval shows the substorms at 18:26 UT and 18:39 UT under study. It is seen that in both events the magnetic disturbances began at the Nurmijarvi station (NUR) (at geomagnetic latitude higher than 56.9°) and then moved poleward to the station Soraja (SOR) (67.3° geomagnetic latitude). It should be noted that in this

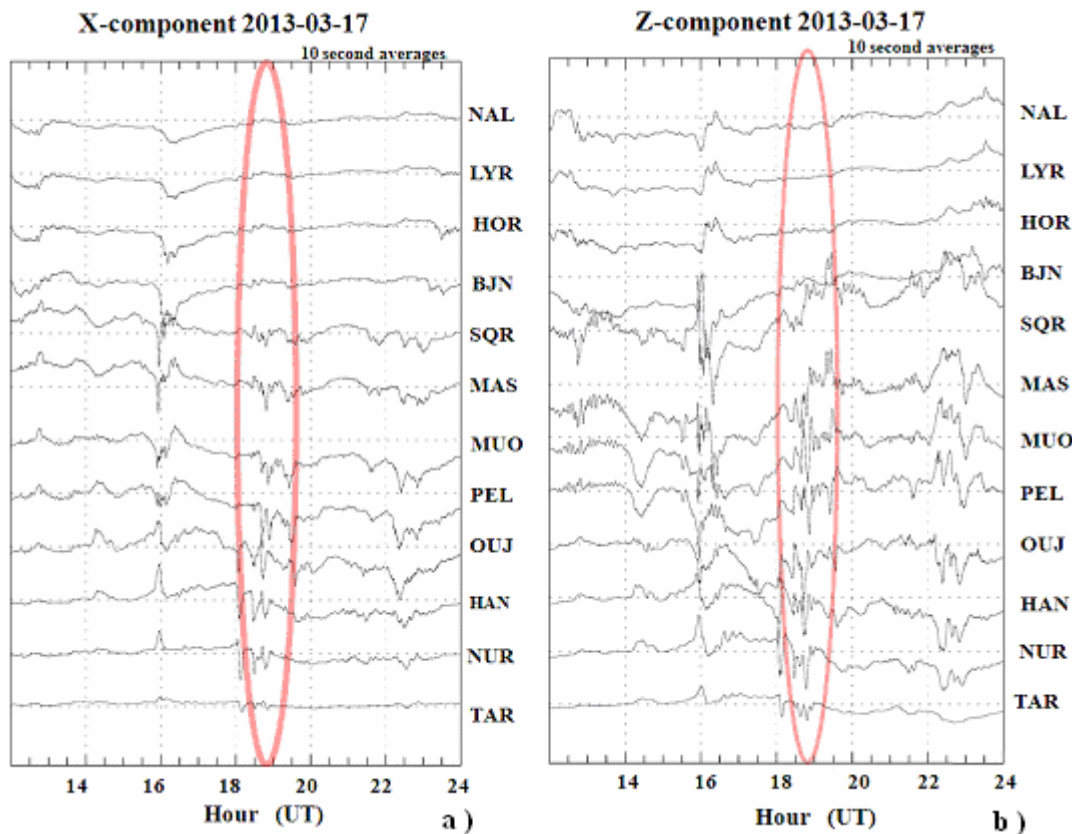


Figure 2 Event on 17 March 2013 - Magnetic cloud. Magnetic field disturbances by IMAGE magnetometer chain are presented. (a) X-components of the magnetic field of the IMAGE TAR-NAL station chain for 17 March 2013 at the 12-24 UT interval; the oval shows the substorms at 18:26 UT and 18:39 UT. (b) Z-components of the magnetic field for 17 March 2013 at the 12-24 UT interval; the oval shows the substorms under study.

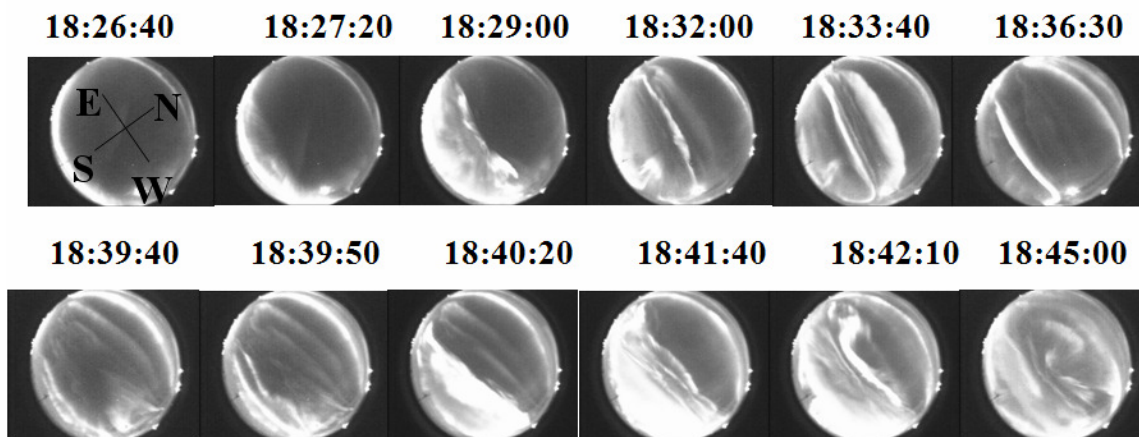


Figure 3 Dynamics of auroras according to the all-sky camera data during two substorms on 17 March 2013. The top panel shows some all-sky camera images taken during the first substorm (from 18:26 to 18:36 UT), the bottom panel shows images from the second substorm (from 18:39 to 18:45 UT). The world directions are marked in the first image, the universal time is written above each image.

day other substorm disturbances were also observed, but they were not registered by the Apatity all-sky camera and for that reason they are not subject of study in this work.

The all-sky camera data on 17 March 2013 are presented in Figure 3. The all-sky camera in Apatity registered the substorm onset at 18:26:40 UT and the second substorm intensification at 18:39:40 UT. In

Figure 3, chosen images of the substorm developments are shown, the world directions are marked in the first image, the universal time is written above each image. The substorm beginning to the South from the station, the arcs movement to the North, reaching the station zenith (18:32 UT) and surpassing it are seen. The second intensification at Apatity begins with an equatorial arc burst at 18:39:40 UT. After that, auroras move toward

zenith, reach it at 18:41:40, and continue moving northward.

Case 2: 14 December 2013

On 14 December 2013, a high speed recurrent stream (HSS) passed by the Earth, and a geomagnetic storm developed. The conditions can be considered as disturbed.

Figure 4 shows the interplanetary conditions taken from the OMNI database for the observation interval 13 -15 December 2013. The Figure 4 format is the same as in Figure 1. The time periods of the high speed stream (HSS) and the region of interaction of HSS with the undisturbed solar wind (CIR) are marked as blue and red crosshatched areas, respectively. The CIR region lasted from 13 UT on 13 December to 02 UT on 14 December, and the high speed recurrent stream – from 02 UT on 14 December to 20 UT on 17 December 2013. The CIR region caused a geomagnetic storm with $D_{st} \sim -40$ nT. The onset times of the substorms observed by IMAGE network and by the all-sky camera are marked by dashed vertical lines.

In Figure 5 the magnetic field disturbances by IMAGE magnetometer chain (TAR-NAL) are presented. The Figure 5 format is the same as in Figure 2. Three substorms were observed during this period: two substorms near D_{st} minimum (at 18:25 UT and 19:57 UT), and one substorm in the recovery phase of the storm (at 22:55 UT). Three ovals show these three substorms in Figure 5. It is seen that in two first events the magnetic disturbances began at the Ouljarvi station (OUJ) (at geomagnetic latitude higher than 60.9°) and then moved poleward to the station Soroja (SOR) (67.3° geomagnetic latitude) and Bear Island (BJN) (71.4° geomagnetic latitude). During the substorm at 22:55 UT the magnetic disturbances began at the Muonio station (MUO) (at geomagnetic latitude higher than 64.7°) and then moved poleward to the station Soroja (SOR) (67.3° geomagnetic latitude). It is noted that Apatity's corrected geomagnetic latitude is $\sim 63.9^\circ$, i.e. it is a bit lower than the latitude of the Muonio station from the IMAGE magnetometer set. It should be mentioned that the observed geomagnetic variations, associated with the auroral electrojets location, correspond well to the position of the auroral oval in disturbed conditions.

In Figure 6 the auroras dynamics according to the all-sky camera data during these 3 substorms of 14 December 2013 is presented. The Figure 6 format is the same as in Figure 3. On 14 December the all-sky camera in Apatity registered three substorms: at 18:25:00 UT, 19:57:10 UT and at 22:55:00 UT. In Figure 6a, 6b and 6c, chosen images of the substorms developments are shown. Two of these three substorms develop by a similar scheme: substorm beginning to the South from the station, arcs movement to the North, reaching the station zenith and surpassing it. The substorm at 22:55:00 UT follows another scheme: substorm beginning to the North from the station, arcs

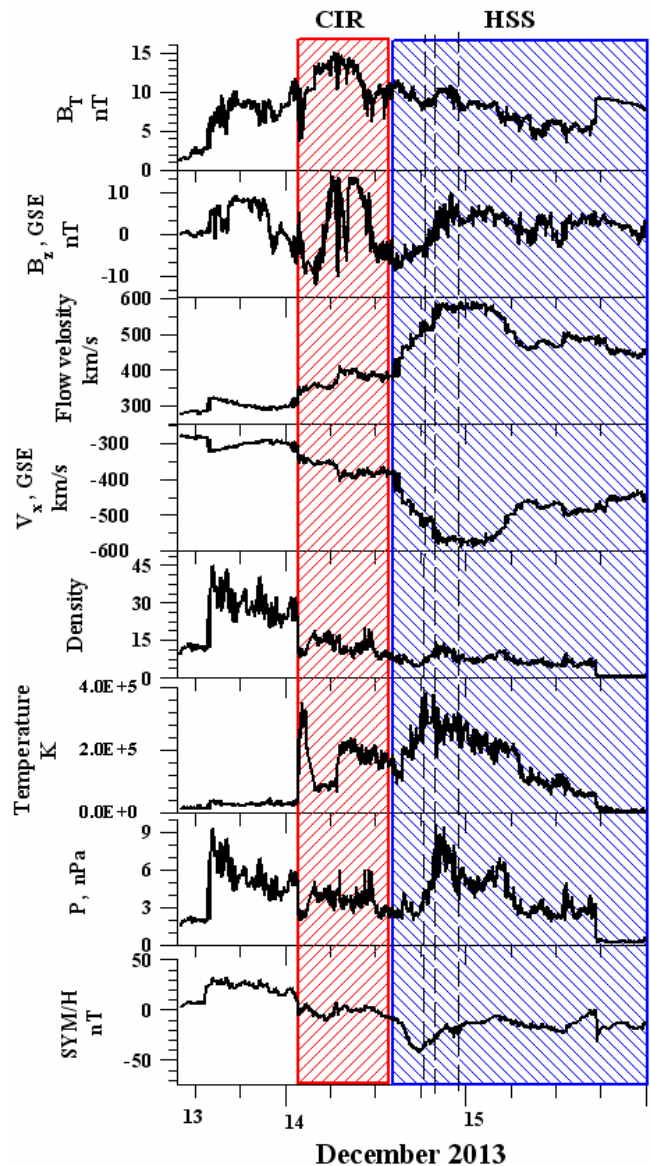


Figure 4 An event on 14 December 2013 - High speed recurrent stream. Solar wind and IMF parameters observations are presented. The Figure 4 format is the same as in Figure 1.

movement to the South, reaching the station zenith and surpassing it. This substorm is observed during the recovery phase of the geomagnetic storm associated with CIR as shown in Figure 4. The substorm onset was to the North of Apatity and only the South part of the substorm is observed from the station.

Case 3: 10.03.2012

On 10 March 2012 quiet conditions were observed in the solar wind.

Figure 7 shows the interplanetary conditions taken from the OMNI database for the observation interval from 09 to 11 March 2012. The Figure 7 format is the same as in Figure 1. It is seen that the end of HSS was observed during 09 March 2012; during this HSS the geomagnetic storm was developed ($D_{st} \sim -150$ nT). But substorms were observed at late recovery phase of this storm, at the end of 10 March 2012. In Figure 7 the

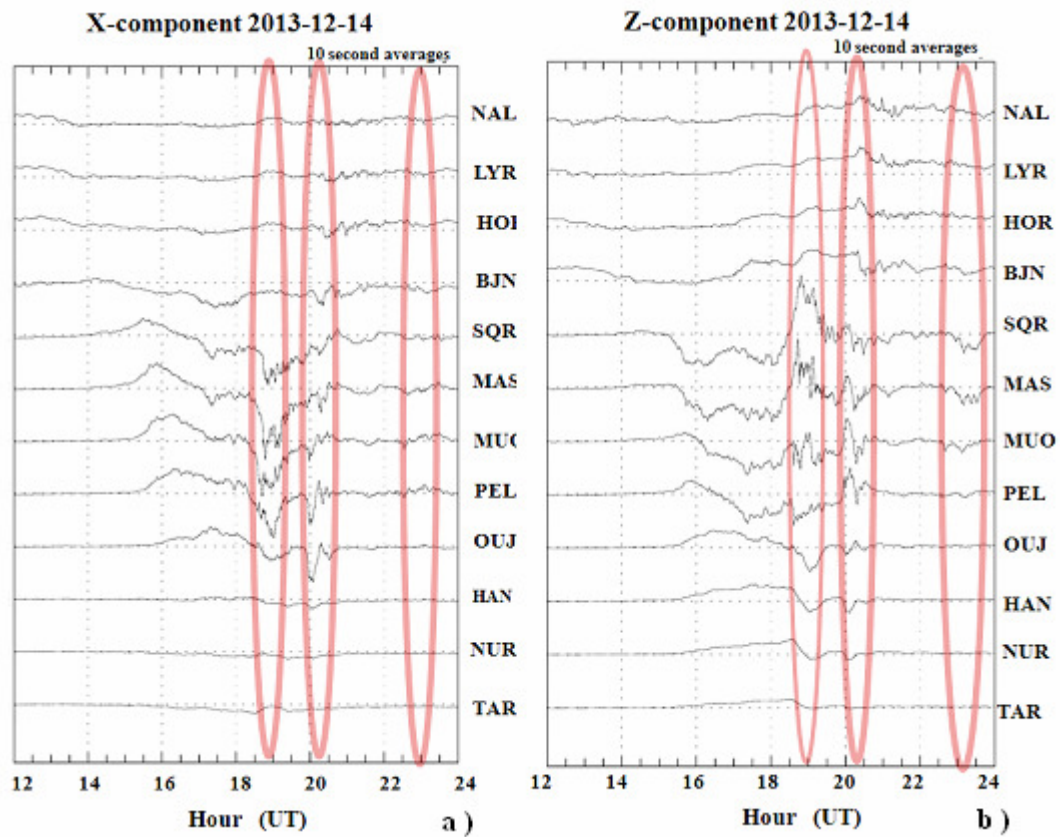


Figure 5 Magnetic field disturbances by IMAGE magnetometer chain for the event 14 December 2013. The Figure 5 format is the same as in Figure 2. Three ovals show three substorms at 18:25 UT, 19:57 UT and 22:55 UT.

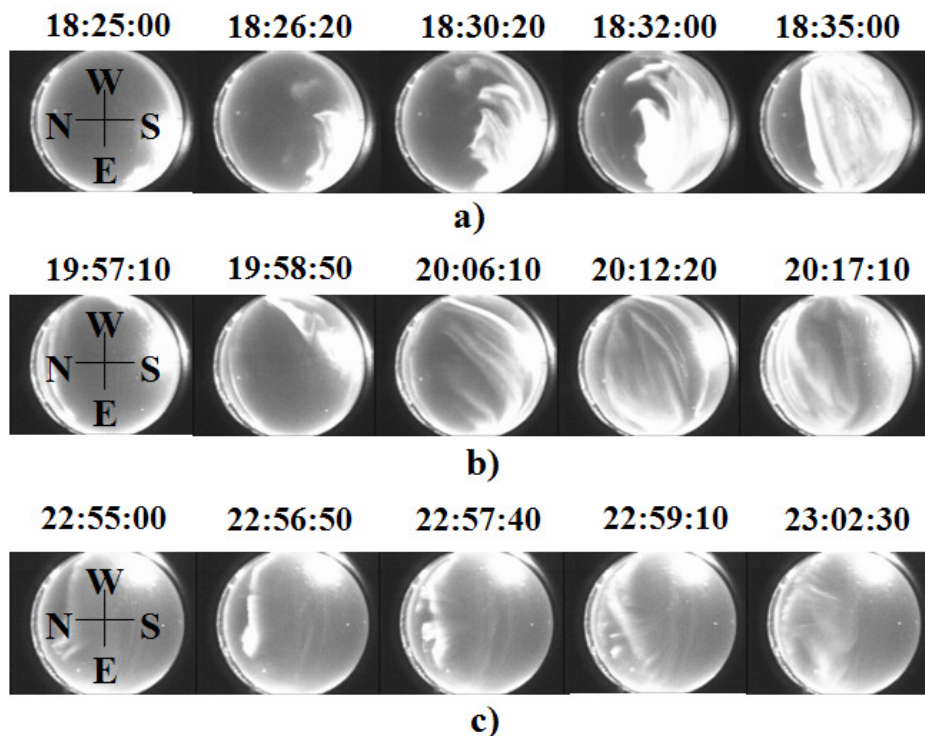


Figure 6 Dynamics of auroras according to the all-sky camera data during 3 substorms on 14 December 2013. The Figure 6 format is the same as in Figure 3. 6(a) - some all-sky camera images from the first substorm (from 18:25:00 to 18:35:00 UT), 6(b) - images from the second substorm (from 19:57:10 to 20:17:10 UT), 6(c) - images from the third substorm (from 22:55:20 to 23:02:30 UT).

onsets of the substorms observed by IMAGE network and by all-sky camera data are marked by dashed vertical lines. It is seen that the substorms occurred under small values of geoeffective parameters (B_z component of the IMF, solar wind velocity etc.), during late recovery phase of storm.

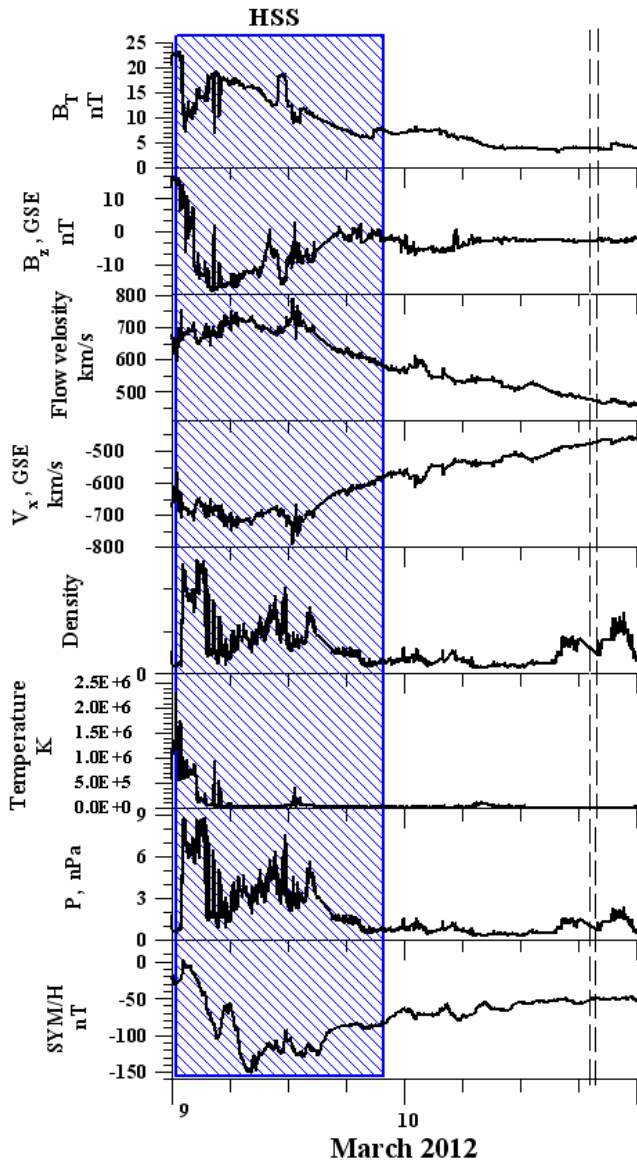


Figure 7 An event on 10 March 2012 - Quiet solar wind conditions. Solar wind and IMF parameters observations are presented. The Figure 7 format is the same as in Figure 1.

In Figure 8 the magnetic field disturbances by IMAGE magnetometer chain (TAR-NAL) on 10 March 2012 from 12 to 24 UT are presented. It is seen that substorms are observed during this period - at 18:33 UT and 18:50 UT. The ovals in Figure 8a and 8b show the substorms at 18:33 UT and 18:50 UT under study.

In Figure 9 the auroras dynamics according to the all-sky camera data during these substorms on 10 March 2012 are presented. The all-sky camera in Apatity registered two substorms at 18:33:00 UT and 18:49:50 UT. In Figure 9, chosen images of the substorm

development are shown. It is seen that the substorm begins to the North from the station, after that the auroras move to the South, reaching the station zenith and surpassing it.

Case 4: 10.04.2013

On 10 April 2013 non-storm, quiet conditions were observed in the solar wind.

Figure 10 shows the interplanetary conditions taken from the OMNI database for the observation interval from 08 to 11 April 2013. The Figure 10 format is the same as in Figure 1. The onset of the substorm observed by IMAGE network and by all-sky camera data is marked by dashed vertical line. It is seen that the substorm occurred during non-storm interval, quiet solar wind conditions.

In Figure 11 the magnetic field disturbances by IMAGE magnetometer chain (TAR-NAL) on 10 April 2013 are presented. The left panel (11a) demonstrates the variations in the X-component of the magnetic field from 12 UT to 23:30 UT; the right panel (11b) shows the variations in the Z-component. It is seen that one substorm is observed during this period - at 21:28 UT.

In Figure 12 the auroras dynamics according to the all-sky camera data during this substorm on 10 April 2013 is presented. The all-sky camera in Apatity registered one substorm at 21:28:00 UT. In Figure 12, chosen images of the substorm development are shown. It is seen that the substorm begins to the North from the station, after that the auroras move to the South, reaching the station zenith and surpassing it. It should be noted that this substorm develops by a scheme similar to the events on 14 December 2013 (at 22:55 UT) and on 10 March 2012 when the substorm onset was also to the North from Apatity and only the development of the South part of the substorm was observed from the station.

Discussion

We investigated substorm developments during storms caused by different sources in the solar wind and during quiet conditions using observations of auroras in Apatity during 2012/2013 winter season. The observations of substorm developments by the all-sky camera in Apatity confirm the typical morphology: in disturbed geomagnetic conditions, when storms are generated, the auroral oval lies at lower latitudes. It is known that under normal conditions (moderate disturbance) the auroral oval is located at geomagnetic latitudes $\sim 65-67^\circ$ ("normal oval"), under quiet conditions, at $B_z > 0$, the auroral oval shrinks and moves to higher latitudes ($> 70^\circ$, "contracted oval"), and in disturbed conditions, at an increase of the value of the IMF negative B_z component the oval expands up to 50° geomagnetic latitude ("expanded oval") (Feldstein and Starkov, 1967). Thus, in quiet conditions Apatity turns out below (equatorward) the auroral oval, and in disturbed conditions - above (poleward) the auroral oval.

Thus the substorm onset in disturbed conditions is located to the South of Apatity and the motion of the

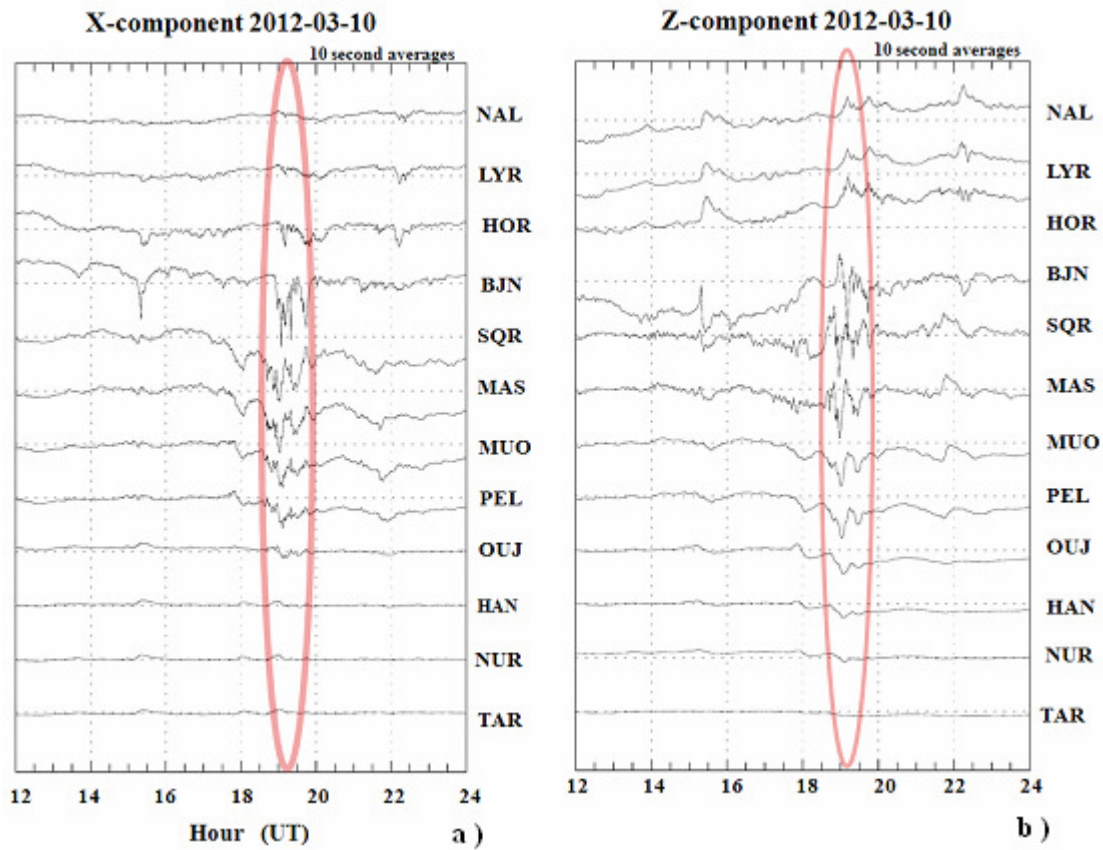


Figure 8 Magnetic field disturbances by IMAGE magnetometer chain for the event 10 March 2012. The Figure 8 format is the same as in Figure 2. The oval shows two substorms at 18:33 UT and 18:49:50 UT.

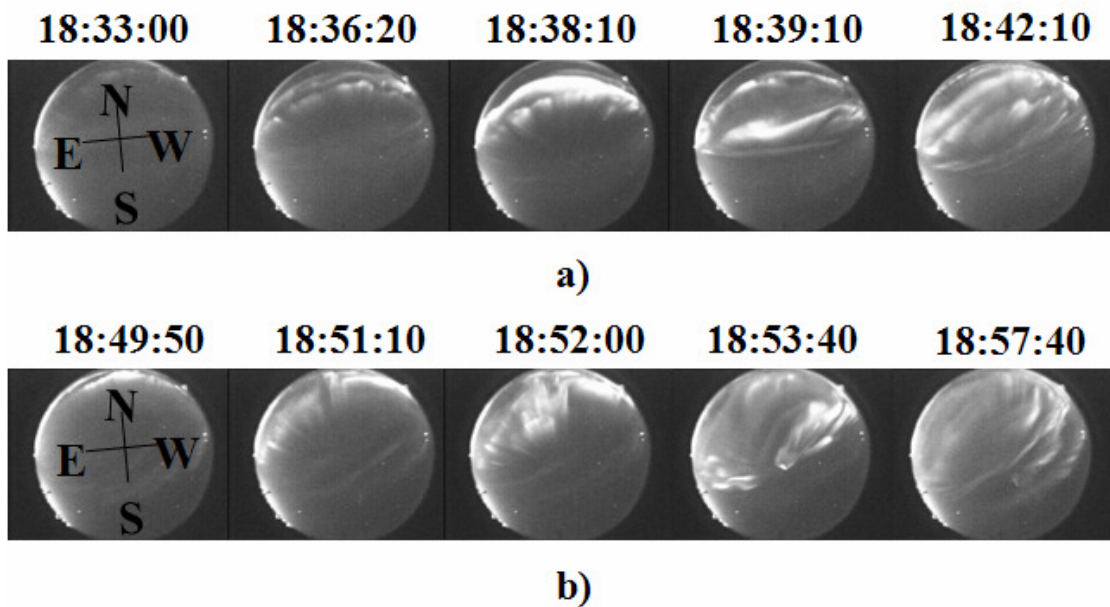


Figure 9 Dynamics of auroras according to the all-sky camera data during two substorms of 10 March 2012. The Figure 9 format is the same as in Figure 3. Chosen all-sky camera images from two substorms from 18:33:00 to 18:42:10 UT (a) and from 18:49:50 to 18:57:40 UT (b) are presented.

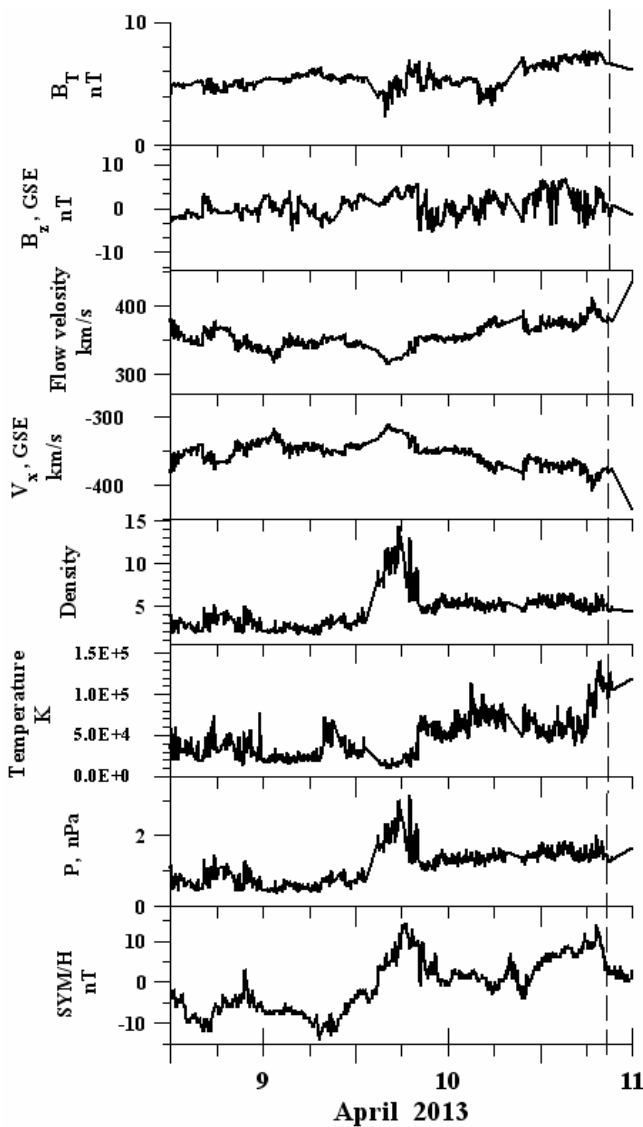


Figure 10 An event on 10 April 2013 - Quiet solar wind conditions. Solar wind and IMF parameters observations are presented. The Figure 10 format is the same as in Figure 1.

polar edge of the substorm bulge can be seen moving in South-North direction over Apatity. This situation was observed mainly for $|D_{st}| > 40nT$. And vice versa,

under quiet conditions or during the recovery phase of a geomagnetic storm, the auroral oval is located at higher latitudes, to the North of Apatity. The substorms arise to the North and during the bulge expansion the movement of the equatorial edge of the auroral bulge in North-South direction can be observed. This situation was observed mainly for $|D_{st}| < 40 nT$.

It should be noted that such research of geomagnetic disturbance development is important for understanding of the regional space weather problems which can be scaled to lower latitudes for higher disturbance levels.

Conclusions

It is shown that 2 types of substorm development occur over Apatity. First type: substorm onset is to the South of Apatity, and the "usual" development of the substorm bulge is seen – from South to North; the polar edge of the bulge is observed to pass over zenith. Second type: the auroral oval is situated at higher latitudes, substorm generates to the North from Apatity, and the movement of the auroras to the South is seen from Apatity, i.e. the equatorial edge of the auroral bulge is observed. It is shown that the first type of substorm development over Apatity happens during geomagnetic storms ($|D_{st}| > 40 nT$), associated with both magnetic clouds and high speed recurrent streams of the solar wind. The second type of substorm development is observed under quiet (non-storm) conditions or during the storm recovery phase ($|D_{st}| < 40 nT$).

Acknowledgements

WIND data used in this study were taken from OMNI through http://cdaweb.gsfc.nasa.gov/cdaweb/istp_public/. We are grateful to J. N. King and N. Papitashvili, the heads of the experiments conducted with these instruments. The paper was partly supported by the RFBR Grants 12-05-01030 and Program #9 of the Presidium of the Russian Academy of Sciences (RAS). The study is also a part of a joint Russian - Bulgarian Project 1.2.10 "Influence" of PGI RAS and IKIT-BAS under the Fundamental Space Research Program between RAS and BAS.

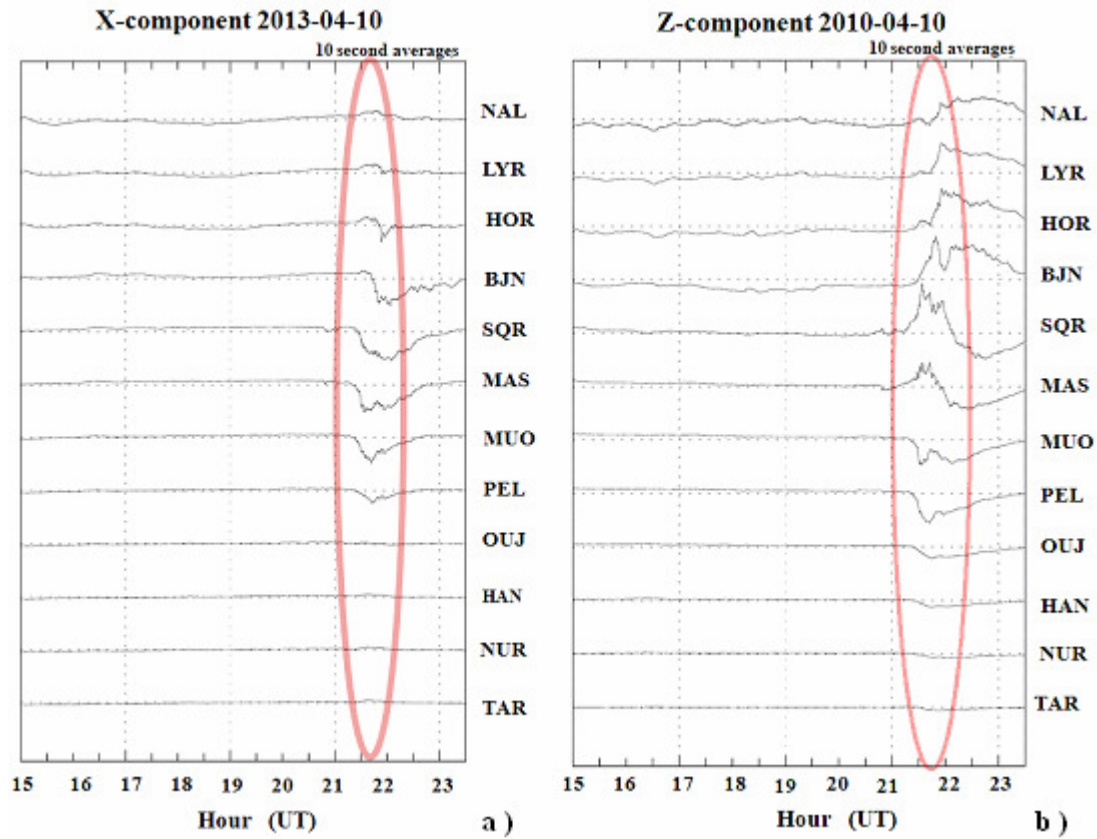


Figure 11 Magnetic field disturbances by IMAGE magnetometer chain for the event 10 April 2013. The Figure 11 format is the same as in Figure 2. The oval shows one substorm at 21:28 UT.

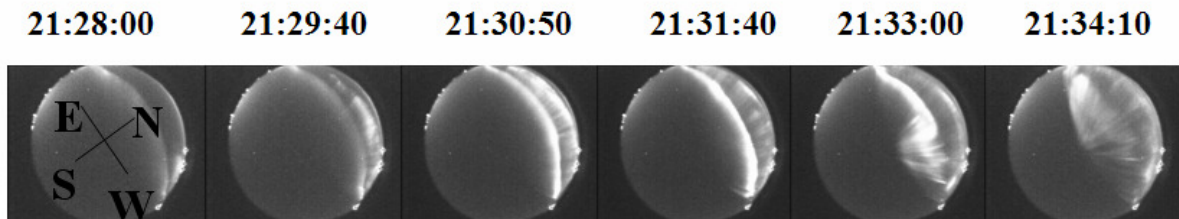


Figure 12 Dynamics of auroras according to the all-sky camera data during one substorm on 10 April 2013. The Figure 12 format is the same as in Figure 3. Chosen all-sky camera images from one substorm from 21:28:00 to 21:34:10 UT are presented.

References

- Akasofu, S. - I.: 1964, *Planet. Space Sci.* 12, 273.
- Akasofu S.I., Wilson C.R., Snyder A.L., Perreault, P.D.: 1971, *Planet. Space Sci.* 19, 477.
- Akasofu S.I., Perreault P.D., Yasuhara F., Meng C.I.: 1973, *J. Geophys. Res.* 78, 7490.
- Akasofu S. I.: 2004, *Space Sci. Rev.* 113, 1.
- Balogh A., Gosling J.T., Jokipii J.R., Kallenbach R., Kunow H.: 1999, *Space Sci. Rev.* 89, 141.
- Burlaga, L.F., Klein, L., Sheeley, N.R., Michels, Jr., Howard, D.J., Koomen, R.A., Schwenn, M.J. and Rosenbauer, H.: 1982, *Geophys. Res. Lett.* 9, 1317.
- Despirak, I.V., Lubchich, A.A., Biernat, H.K., Yahnin, A.G.: 2008, *Geomagn. Aeronomy* 48(3), 284.
- Despirak, I.V., Lubchich, A.A., Yahnin, A.G., Kozelov, B.V., Biernat, H.K.: 2009, *Ann. Geophys.* 27, 1951.
- Despirak, I.V., Lyubchich, A.A., Kleimenova, N.G.: 2014, *Geomagn. Aeronomy* 54(5), 575.
- Gerard, J.-C., Hubert, B., Grard, A., Meurant, M.: 2004, *J. Geophys. Res.* 109, A03208, doi: 10.1029/2003JA010129.
- Doolittle J.H., Mende S.B., Frey H.U., Rosenberg T.J., Weatherwax A.T., Lanzerotti L.J., et al.: 1998, *Proc. 4th Int. Conf. on Substorms*, March 9-13, 1998, Japan, 47.
- Feldstein Y.L., Starkov G.V.: 1967, *Planet. Space Sci.* 15, 209.
- Gupta J.C., Loomer E.I.: 1979, *Planet. Space Sci.* 27, 1019.
- Gussenhoven M.S.: 1982, *J. Geophys. Res.* 87, 2401.
- Kisabeth J.L., Rostoker G.: 1974, *J. Geophys. Res.* 79, 972.
- Klein L.W., Burlaga L.F.: 1982, *J. Geophys. Res.* 87, 972.
- Kozelov, B.V., Pilgaev, S.V., Borovkov, L.P., Yurov, V.E.: 2011, in N.V. Semenova, A.G. Yahnin (ed.), *Physics of auroral phenomena, Apatity, Russia*, p. 129, <http://pgia.ru:81/seminar/archive/>.
- Kozelov, B.V., Pilgaev, S.V., Borovkov, L.P., Yurov, V.E.: 2012, *Geosci. Insrum. Method. Data Syst.* 1, 1.
- Kuznetsov S., Lazutin L.L., Rosenberg T., Borovkov L., Gotselyuk Yu., Weatherwax A.: 2001, *Proc. 5th Int. Conf. on Substorms*, St. Petersburg, Russia, 511.
- Loomer E.I., Gupta J.C.: 1980, *J. Atmos. Sol.-Terr. Phys.* 42, 645.
- Lui A.T.Y., Anger C.D., Akasofu S.I.: 1975, *J. Geophys. Res.* 80, 3603.
- Lui A.T.Y., Akasofu S.I., Hones E.W., Jr., Bame S.J., Mclwan C.E.: 1976, *J. Geophys. Res.* 81, 1415.
- Mende S.B., Frey H.U., Geller S.P., Doolittle J.H.: 1999, *J. Geophys. Res.* 104, 2333.
- Petrukovich A.A., Baumjohann W., Nakamura R., Mukai T., Troshichev O.A.: 2000, *J. Geophys. Res.* 105, 21109.
- Sergeev, V.A., Yahnin, A.G., Dmitrieva, N.P.: 1979, *Geomagn. Aeron.* 19, 1121.
- Troshichev O.A., Kuznetsov B.M., Pudovkin, M.I.: 1974, *Planet. Space Sci.* 22, 1403.
- Tsurutani B.T., Gonzalez W.D., Gonzalez A.L.C., et al.: 2006, *J. Geophys. Res.* 111, A07S01. doi: 10.1029/2005JA011273.
- Vorobjev, V.G., Zverev, W.L.: 1982, *Geomagn. Aeron.* 22(1), 81.
- Weatherwax A.T., Rosenberg T.J., MacLennan C.G., Doolittle J.H.: 1997, *Geophys. Res. Lett.* 24, 579.
- Wiens R.G., Rostoker G.: 1975, *J. Geophys. Res.* 16, 2109.
- Yahnin, A.G., Despirak, I.V., Lyubchich, A.A. and Kozelov B.V.: 2004, in N. Ganushkina and T. Pulkkinen (eds.), *Solar wind control of the auroral bulge expansion*, Finnish Meteorological Institute, Helsinki, Finland, p. 31.
- Yermolaev, Yu.I., Yermolaev, M.Yu.: 2006, *Adv. Space Res.* 37(6), 1175.
- Yermolaev Yu.I., Nikolaeva N.S., Lodkina I.G., Yermolaev M.Yu.: 2009, *Cosmic Research (Engl. Transl.)*, 47, 81.